JOURNAL OF AIRCRAFT
Vol. 35, No. 3, May–June 1998

Incorporating Flight Data into a Robust Aeroelastic Model

Rick Lind* and Marty Brenner†
NASA Dryden Flight Research Center, Edwards, California 93523-0273

Stability analysis and control synthesis for high-performance aircraft must account for errors in the aircraft model. This paper introduces a method to update a theoretical model using measured flight data. Variations between the flight data and model are represented as uncertainty operators in a robust stability framework. The structured singular value can directly account for these uncertainty operators to compute stability margins robust to the associated dynamical variations. This procedure is used to formulate an uncertain model of an F/A-18 fighter aircraft and compute stability margins that indicate the worst-case flutter conditions.

Nomenclature

C = damping matrix
K = stiffness matrix
M = mass matrix
Q = unsteady aerodynamic forces
$\bar{q}$ = dynamic pressure
W = weight for input multiplicative uncertainty
Δ = uncertainty matrix
δ = uncertainty scalar
μ = structured singular value
$\bar{\sigma}$ = maximum singular value

Introduction

AIRCRAFT stability, particularly for high-performance aircraft, may be extremely sensitive to aircraft dynamics and flight conditions. Analytical models must be accurate to ensure that the estimated stability properties represent the true aircraft stability properties. Such accuracy is difficult to achieve for complex modern aircraft designs because of components, such as flexible structural elements, and flight regimes, such as high angle-of-attack and transonic operating conditions.

It is essential to incorporate flight data into the model development process because this data provides the only true indication of the actual aircraft dynamics. This data will generally not match identically with the predicted data from an analytical model, and so the model must be updated to reflect the dynamics observed by the measurements.

A straightforward method of generating a model from the flight data is to identify a system model entirely from the measurements using standard system identification algorithms.[1] Direct application of these methods to aeroelastic systems rarely produces an accurate model that accounts for the dynamics of the aircraft.[2] The methods are often unable to utilize aeroelastic flight data that are typically of poor quality relative to ground vibration test data because of the low signal-to-noise ratio (SNR) and low observability of some dynamics in the response measurements.

An alternative method is to utilize a nominal model as an initial estimate to represent the true aircraft and use flight data to update specific elements of this model.[3] Parameter estimation algorithms may be used to compute these specific elements, but problems are often encountered when using noisy measured flight data to estimate parameters of a realistically complex model.

This paper introduces a method of incorporating flight data into the model development process through uncertainty operators for a system expressed in a robust stability framework. These uncertainty operators are associated with a model to describe levels of errors and unmodeled dynamics using linear fractional transformation (LFT) relationships.[4] The structured singular value is used to compute a robust stability measure of the aeroelastic model with respect to these uncertainty operators.[5]

The procedure is demonstrated by incorporating flight data from an F/A-18 aircraft into a theoretical model to develop a set of uncertainty operators that accounts for variations between the data and the model over a range of flight conditions. Robust flutter margins are computed with respect to this uncertainty description to indicate aeroelastic instabilities that may lie closer to the flight envelope than previously predicted using only the theoretical model.

Robust Stability μ Framework

Robust Stability

Robust stability considers the characteristics of a system model under the influence of perturbations. These perturbations might represent unmeasured forces acting on the system or errors and unmodeled dynamics associated with the model. Often the exact value of these perturbations is not known, but a range of magnitudes and phases for a set of perturbations can be anticipated. Each perturbation is considered an uncertainty that is described by an operator, Δ, and is contained in a set, $\mathbf{\Delta}$, which is norm bounded to reflect limits on the range of anticipated perturbation sizes:

$$\mathbf{\Delta} = \{\Delta: \|\Delta\|_\infty \leq 1\} \tag{1}$$

These uncertainty operators are formulated to affect the system in a feedback manner as in Fig. 1. This type of relationship is a linear fractional transformation that allows multiple systems and uncertainties to be represented as a plant with an associated structured uncertainty operator.

The robust stability of P with respect to the set $\mathbf{\Delta}$ can be guaranteed if $\|P\|_\infty < 1$ as proved by the small gain theorem.[6] This condition is sufficient but not necessary because it may be overly conservative with respect to structured uncertainty. The structured singular value μ is defined for P as a measure of robustness with respect to $\mathbf{\Delta}$.[5]

$$\mu(P) = \frac{1}{\min_{\Delta \in \mathbf{\Delta}} \{\bar{\sigma}(\Delta): \det(I - P\Delta) = 0\}} \tag{2}$$

Received Jan. 2, 1997; revision received Oct. 28, 1997; accepted for publication Nov. 28, 1997.

*NRC Postdoctoral Research Fellow, M/S 4840D/RS. E-mail: rick.lind@dfrc.nasa.gov. Member AIAA.

†Research Engineer, M/S 4840D/RS. E-mail: martin.brenner@dfrc.nasa.gov. Member AIAA.

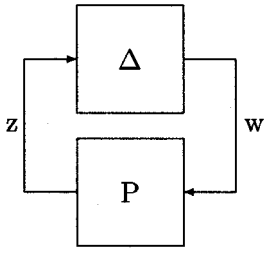

Fig. 1 Block diagram for robust stability analysis using μ.

with $\mu = 0$ if no $\Delta \in \mathbf{\Delta}$ exists such that $\det(I - P\Delta) = 0$. μ is an exact measure of robustness for systems with structured uncertainty. The inverse of μ can be interpreted as the magnitude of the smallest destabilizing perturbation $\Delta \in \mathbf{\Delta}$. Thus, the system P is guaranteed to be robustly stable with respect to the entire unity norm bounded set $\mathbf{\Delta}$ if $\mu(P) < 1$.[5]

Model Validation

The robustness measured by μ is truly meaningful only if it is computed with respect to a realistic uncertainty description. Too much uncertainty may cause the robustness measure to be overly conservative, whereas too little uncertainty may generate a robustness measure that does not consider the true errors in the model.

Experimental flight data can be used to determine some measure of realism for the uncertainty description. Model validation algorithms are formulated that indicate if the range of plant measurements admitted by the uncertainty operators encompass the data measurements. A finite amount of data can never completely validate a model, and so the model is said to be not invalidated if the data measurements fall within the upper and lower bounds of the theoretical measurements as determined by the range of uncertainty perturbations.

This paper uses a μ-based model validation algorithm that can be directly used for analysis of robust aeroelastic models.[7] This method assumes that the theoretical plant model P and associated uncertainty set $\mathbf{\Delta}$ are known. The plant has an input for disturbances and output for measurements along with a vector input and output to relate P with $\mathbf{\Delta}$. Define P_{11} as the transfer function from uncertainty input and output vectors that was used for stability analysis in Fig. 1. Define P_{22} as the transfer function from disturbance to measurements for the nominal plant model. Define also off-diagonal plant elements P_{12} and P_{21} to relate all input and output signals. Consider the relationship between the input u and measurement y for this formulation [4]:

$$0 = [P_{22}u - y] + P_{21}\Delta(I - P_{11}\Delta)^{-1}[P_{12}u] \tag{3}$$

$$0 = \bar{P}_{22} + P_{21}\Delta(I - P_{11}\Delta)^{-1}\bar{P}_{12} \tag{4}$$

This equation is similar to a robust stability condition for an LFT involving Δ and a plant $\bar{P}$ determined by the matrices $\{P_{11}, \bar{P}_{12}, P_{21}, \bar{P}_{22}\}$. The existence of an Δ that satisfies these equations is equivalent to the plant not being robustly stable. Thus, the model is not invalidated by the flight data if $\mu(\bar{P}) > 1$. An equivalent condition using a matrix of lower dimension is formulated such that the following condition is satisfied if the model is not invalidated[7]:

$$\mu(P_{11} - \bar{P}_{12}\bar{P}_{22}^{-1}P_{21}) > 1 \tag{5}$$

Nominal Aeroelastic Model

Consider the generalized aeroelastic equation of motion[8]:

$$M\ddot{\boldsymbol{\eta}} + C\boldsymbol{\eta} + K\boldsymbol{\eta} + \bar{q}Q\boldsymbol{\eta} = 0 \tag{6}$$

Define $\boldsymbol{\eta} \in R^n$ as the generalized coordinate vector. For a system with n modes, define $M \in R^{n\times n}$ as the mass matrix, $C \in R^{n\times n}$ as the damping matrix, and $K \in R^{n\times n}$ as the stiffness matrix. $\bar{q} \in R$ is a scalar representing the dynamic pressure and $Q \in C^{n\times n}$ is the frequency varying matrix of unsteady aerodynamic forces.

The unsteady aerodynamic forces are usually computed at distinct frequencies, but a $Q(s)$ may be expressed as a continuous function of frequency using several analytical formulations. A general form for $Q(s)$ that encompasses these formulations is a finite dimensional, linear time-invariant state-space model determined by the quadruple $Q(s) = \{A_Q, B_Q, C_Q, D_Q\}$.

The equations of motion may be expressed as a state-space system with the generalized states $\boldsymbol{\eta}$ and unsteady aerodynamic force states $\boldsymbol{x}$. The state update is determined by these differential equations[9]:

$$\begin{bmatrix}\boldsymbol{\eta}\\ \dot{\boldsymbol{\eta}}\\ \boldsymbol{x}\end{bmatrix} = \begin{bmatrix}0 & I & 0\\ -M^{-1}(K + \bar{q}D_Q) & -M^{-1}C & -\bar{q}M^{-1}C_Q\\ B_Q & 0 & A_Q\end{bmatrix}\begin{bmatrix}\boldsymbol{\eta}\\ \boldsymbol{\eta}\\ \boldsymbol{x}\end{bmatrix} \tag{7}$$

Uncertainty in Aeroelastic Models

Parametric Uncertainty Associated with Model

Parametric uncertainty denotes operators that are associated with specific parameters in the system model. This type of uncertainty is useful to describe modeling errors in the finite element structural model and the unsteady aerodynamic force representation.

Define an operator $\Delta_K \in R^{n\times n}$ that describes additive uncertainty of a nominal stiffness matrix K_0. Associate a weighting matrix $W_K \in R^{n\times n}$ with this uncertainty such that the stability analysis should consider all stiffness variations described by $\|\Delta_K\|_\infty \le 1$:

$$K = K_0 + W_K\Delta_K \tag{8}$$

The uncertainty operator can be associated with P in a feedback manner by substituting K into the update law of Eq. (7) and extracting Δ_K:

$$\ddot{\boldsymbol{\eta}} = -M^{-1}(K_0 + W_K\Delta_K + \bar{q}D_Q)\boldsymbol{\eta} - M^{-1}C\boldsymbol{\eta} - \bar{q}M^{-1}C_Q\boldsymbol{x} \tag{9}$$

$$\ddot{\boldsymbol{\eta}} = [-M^{-1}(K_0 + \bar{q}D_Q)\boldsymbol{\eta} - M^{-1}C\boldsymbol{\eta} - \bar{q}M^{-1}C_Q\boldsymbol{x}] - \Delta_K[M^{-1}W_K\boldsymbol{\eta}] \tag{10}$$

$$\ddot{\boldsymbol{\eta}} = [-M^{-1}(K_0 + \bar{q}D_Q)\boldsymbol{\eta} - M^{-1}C\boldsymbol{\eta} - \bar{q}M^{-1}C_Q\boldsymbol{x}] - \Delta_K\boldsymbol{z}_K \tag{11}$$

$$\ddot{\boldsymbol{\eta}} = [-M^{-1}(K_0 + \bar{q}D_Q)\boldsymbol{\eta} - M^{-1}C\boldsymbol{\eta} - \bar{q}M^{-1}C_Q\boldsymbol{x}] - \boldsymbol{w}_K \tag{12}$$

The signals $\boldsymbol{z}_K$ and $\boldsymbol{w}_K$ are introduced to relate the nominal dynamics and the uncertainty Δ_K. The signal $\boldsymbol{z}_K = M^{-1}W_K\boldsymbol{\eta}$ is a plant output and the signal $\boldsymbol{w}_K = \Delta_K\boldsymbol{z}_K$ is the input signal through which the uncertainty affects the state update.

Parametric uncertainty can also be associated with elements of the unsteady aerodynamic forces. Define an operator $\Delta_{A_Q} \in R^{n_Q\times n_Q}$ to describe multiplicative uncertainty in the nominal state matrix A_{Q_0} of $Q(s)$. Include a weighting $W_{A_Q} \in R^{n_Q\times n_Q}$ such that the range of anticipated errors in A_Q is described by all Δ_{A_Q} with $\|\Delta_{A_Q}\|_\infty \le 1$:

$$A_Q = A_{Q_0}(I + W_{A_Q}\Delta_{A_Q}) \tag{13}$$

This uncertainty can also be associated with the system in a feedback manner by substituting A_Q into Eq. (7) and extracting Δ_{A_Q}:

$$\boldsymbol{x} = B_Q\boldsymbol{\eta} + A_{Q_0}(I + W_{A_Q}\Delta_{A_Q})\boldsymbol{x} \tag{14}$$

$$\boldsymbol{x} = [B_Q\boldsymbol{\eta} + A_{Q_0}\boldsymbol{x}] + \Delta_{A_Q}[W_{A_Q}A_{Q_0}\boldsymbol{x}] \tag{15}$$

$$\boldsymbol{x} = [B_Q\boldsymbol{\eta} + A_{Q_0}\boldsymbol{x}] + \Delta_{A_Q}\boldsymbol{z}_{A_Q} \tag{16}$$

$$\boldsymbol{x} = [B_Q\boldsymbol{\eta} + A_{Q_0}\boldsymbol{x}] + \boldsymbol{w}_{A_Q} \tag{17}$$

Additional signals are again introduced to relate the nominal dynamics and the uncertainty where $\boldsymbol{z}_{A_Q} = W_{A_Q}A_{Q_0}\boldsymbol{x}$ is a plant output and the signal $\boldsymbol{w}_{A_Q} = \Delta_{A_Q}\boldsymbol{z}_{A_Q}$ is an input.

The state-space plant is formulated using these additional input and output signals to fit the LFT model of Fig. 1. The uncertainty operator Δ of this figure is structured to be block diagonal with Δ_K and Δ_{A_Q} along the diagonal:

$$\begin{bmatrix} \boldsymbol{\eta} \\ \dot{\boldsymbol{\eta}} \\ \dot{\boldsymbol{x}} \\ \hline \boldsymbol{z}_K \\ \boldsymbol{z}_{A_Q} \end{bmatrix} = \left[\begin{array}{ccc|cc} 0 & I & 0 & 0 & 0 \\ -M^{-1}(K_0 + \bar{q}_0 D_Q) & -M^{-1}C & -\bar{q}_0 M^{-1}C_Q & -I & 0 \\ B_Q & 0 & A_{Q_0} & 0 & I \\ \hline M^{-1}W_K & 0 & 0 & 0 & 0 \\ 0 & 0 & W_{A_Q}A_{Q_0} & 0 & 0 \end{array}\right] \begin{bmatrix} \boldsymbol{\eta} \\ \dot{\boldsymbol{\eta}} \\ \dot{\boldsymbol{x}} \\ \hline \boldsymbol{w}_K \\ \boldsymbol{w}_{A_Q} \end{bmatrix} \tag{18}$$

Other parameters of the equations of motion can be affected by uncertainty in a manner similar to K and A_Q. The choice of uncertainties Δ_K and Δ_{A_Q} was chosen here to illustrate the procedure of introducing parametric uncertainty, but the actual choice of parametric uncertainty operators is problem dependent and varies with model accuracy.

Dynamic Uncertainty Associated with Model

Dynamic uncertainty operators are often associated with aeroelastic models to account for modeling errors that are not efficiently described by parametric uncertainty. Unmodeled dynamics and inaccurate mode shapes are examples of modeling errors that can be described with less conservatism by dynamic uncertainties than with parametric uncertainties. These dynamic uncertainties are typically complex to represent errors in both magnitude and phase of signals.

For example, consider a system P_{true} having two modes with natural frequencies at 4 and 30 rad/s:

$$P_{\text{true}} = \left(\frac{16}{s^2 + 0.4s + 16}\right)\left(\frac{900}{s^2 + 0.6 + 900}\right) \tag{19}$$

Define a nominal model P_0 that will be used for stability analysis of the system but does not model the high-frequency mode of P_{true}:

$$P_0 = \frac{16}{s^2 + 0.4s + 16} \tag{20}$$

The large difference in natural frequency between the high- and low-frequency modes of P_{true} precludes parametric uncertainty associated with the low-frequency mode of P_0 to be a reasonable description of the modeling errors in P_0. The magnitude of any parametric uncertainty associated with the low-frequency mode would need to be extremely large to account for the unmodeled high-frequency dynamics, and so the stability analysis would be relatively meaningless because the large uncertainty would imply that the plant is not accurate at any frequencies.

A multiplicative uncertainty operator $\Delta_m \in C$ can be used to describe the high-frequency modeling error without introducing the excessive conservatism resulting from a parametric uncertainty description. Associate a complex scalar weighting function $W_m \in C$ with this uncertainty to reflect the frequency-varying levels of modeling errors:

$$W_m = 100\,\frac{s + 0.5}{s + 500} \tag{21}$$

The multiplicative uncertainty affects the plant by the relationship $P = P_0(I + W_m\Delta_m)$. Figure 2 presents the magnitude of the transfer function from input to output for P_{true} and P_0 along with the maximum magnitude of $|P_0(I + W_m\Delta_m)|$, which is an upper bound for the output of the uncertain plant at each frequency. The dynamic uncertainty is able to bound the modeling error near the high-frequency mode without introducing excessive conservatism from large uncertainty associated with the low-frequency mode.

Uncertainty Associated with Flight Data

A theoretical model with an associated uncertainty description may be an accurate representation of the aeroelastic dynamics of an aircraft even though responses from that model may not identically match flight data. Additional uncertainties can be associated with the model to describe errors observed between the predicted and measured responses from a commanded excitation to the aircraft. These uncertainties do not necessarily indicate errors in the model; rather, they indicate errors in the process used to generate aeroelastic responses and measure flight data.

One source of error is an incorrect assumption of excitation force used to generate the predicted and measured responses. The measured excitation force associated with the flight data may not correctly account for poor hardware performance and nonuniform spectral distribution of the force. Also, inexactly phased excitation between multiple-force mechanisms may excite modes that are not anticipated by a theoretical analysis. A frequency-varying dynamic uncertainty can be associated with the force input of the analytical model to describe errors in the excitation.

The phenomenon of nonrepeatability can cause discrepancies between predicted and measured responses from multiple

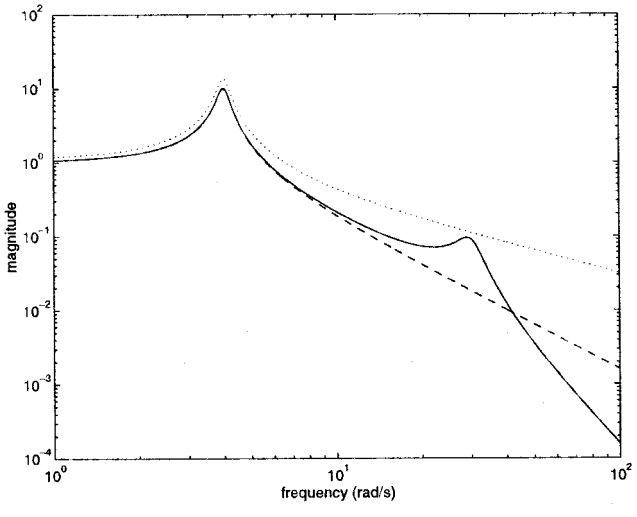

Fig. 2 Transfer functions for example system with multiplicative uncertainty: plant p_{true} (——), nominal plant P_0 (– – –), maximum $|P_0(I + W_m\Delta_m)|$ at each frequency (· · ·).

occurrences of excitation signals. Nonrepeatability affects flight data by introducing slight variations in responses, even for data recorded at identical flight conditions with identical excitation signals. This unexplained behavior may result from some unmodeled nonlinear dynamic or inexact excitation that is incorrectly measured. For example, external disturbances such as wind gusts or turbulence may introduce an unmodeled dynamic that inconsistently affects the aircraft responses. A frequency-varying dynamic uncertainty may be associated with the model to describe nonrepeatable data variations.

Another source of error between predicted and measured responses is an incorrect assumption of flight condition. Flight data sets are sometimes generated at test points that attempt to maintain a constant flight condition to match the data sets predicted from a model describing the aeroelastic dynamics at that same flight condition. Slight variations in flight conditions while the experimental response is measured may cause some discrepancy between the predicted response and the flight data. Parametric uncertainty associated with the unsteady aerodynamic model can be used to account for these errors because flight condition variations only affect the aerodynamic model and not the structural model.

The model may accurately represent the mode shapes of the aircraft but have a poor representation of the sensor locations. The responses measured by sensors are inherently dependent on their location with respect to mode shapes to determine the magnitude and phase of the signal. A frequency-varying dynamic uncertainty can be associated with the output of the plant model to describe errors in both mode shape and sensor location predictions.

The choice of signal-processing algorithms can also introduce errors between predicted and measured responses. The Fourier transform, which is the traditional tool for signal processing, assumes several characteristics of the data that may be violated with transient response aeroelastic data. Parametric uncertainty associated with the modal parameters of the linear model may be used to describe some errors in the natural frequency and damping estimations, whereas dynamic uncertainty may also be required to describe errors introduced by leakage and aliasing effects.

Procedure to Incorporate Flight Data

Model Updating

The procedure developed in this paper to incorporate flight data into an aeroelastic model performs a model update rather than a model identification. An update assumes a nominal model is known from theoretical analysis and the flight data are used to change elements in that model, whereas an identification generates the nominal model entirely from the flight data.

A model in the μ framework has a nominal dynamics model and an uncertainty description that can be updated. The dynamics model can be difficult to update because of numerous elements and modes, and so an alternative approach is to update only the uncertainty description. This approach may be conservative if the nominal dynamics model has large errors, but it may be advantageous if that model is nearly accurate and the data show some variations in observed dynamical properties.

The updating of the uncertainty description can be accomplished using the model validation criterion of Eq. (5). This criterion determines if the uncertainty levels are sufficient to describe differences between the model and measurements such that the data do not invalidate the model. The μ value used in Eq. (5) determines the amount of conservatism in the model because a μ much greater than 1 indicates too much uncertainty is present, whereas a μ much less than 1 indicates too little uncertainty is present.

An iterative μ method approach is formulated that generates a reasonable uncertainty description ensuring that the model is not invalidated while reducing the conservatism. A model validation check is repeated using a set of flight data for models with differing levels of uncertainty until μ for Eq. (5) is only slightly greater than 1. The update law for the uncertainty levels can be a simple division by μ to either decrease or increase the amount of uncertainty depending on the conservatism measured by μ from the model validation condition.

This update method can be compared to a parameter estimation method because both methods make assumptions on the knowledge of a nominal plant. The main difference is that parameter estimation methods only assume a structure for the unknown elements of the plant and rely entirely on the data to provide magnitudes for these structured elements. The update method assumes both a structure and initial estimate for every element of the plant and uses the flight data to improve, if possible, on the structured elements.

The μ method developed here using the update procedure has several advantages as compared to either system identification or parameter estimation methods. One advantage is the ability to utilize poor-quality flight data with low SNR. Because the model is only updated through a validation procedure, poor-quality data may not observe the dynamics sufficiently to indicate errors between the model and the data, so that the uncertainty description may be overly optimistic. System identification and parameter estimation methods rely entirely on the data to generate a model; therefore, poor-quality data have a much stronger negative effect on these methods.

Another advantage to this μ method is the inherent concept of a set of plant models resulting from the set of uncertainty perturbations. The physical aircraft may be time-varying because of mass consumption and other factors, and so a single plant model derived from traditional methods cannot capture this effect. The uncertain model in the μ framework can bound the range of time-varying dynamics to ensure the model represents different dynamical behaviors of the aircraft over a range of flight conditions and durations.

Approaches to Utilize Flight Data

A flight test will generally consist of maneuvers at several test points that may be at identical or different flight conditions. The entire flight test program will utilize many flight tests to measure response data at test points throughout the flight envelope. Several approaches are formulated to utilize multiple flight datasets to update the uncertainty description associated with a nominal plant model. The uncertainty description may be different for each approach and the resulting flutter margin will be different for each approach because of the dependence of μ on the uncertainty set. Two approaches discussed here are denoted as local and global.

A local approach utilizes flight data from test points at identical flight conditions to generate an uncertainty description for the nominal model at the particular flight condition associated with the data. The magnitude of the uncertainty operators is chosen such that a robust model at the single flight condition is not invalidated by any of the flight data sets measured at that same flight condition with no consideration of data from other flight conditions.

The local approach presents the benefit of independently computing uncertainty descriptions for models at different flight conditions. This allows each uncertainty description to be less conservative because, for example, more uncertainty may be required to validate models at transonic conditions than at subsonic conditions.

A global approach utilizes the entire set of flight data from test points throughout the flight envelope to generate a single uncertainty description for all nominal aircraft models. The magnitudes of the uncertainty operators are chosen such that all nominal models with the associated uncertainty description are not invalidated by any of the flight data sets.

There are several advantages and disadvantages to using the global approach as compared to the local approach. A disad-

vantage is a possible large increase in conservatism of the flutter margin because the uncertainty description is not minimized at each flight condition. A single particularly inaccurate plant model will require large uncertainty operators that may be highly conservative for plant models at flight conditions that are better representations of the true dynamics.

The advantage to this approach, however, is that the uncertainty description is truly worst-case with respect to the entire flight envelope. The worst-case errors from the worst-case flight condition are used to generate the uncertainty description for all conditions. Also, this approach is less sensitive to poorly measured flight data. A poorly modeled modal response may only appear in certain data sets. The local approach would not include uncertainty for these dynamics at conditions that did not clearly observe this modal response, and so the resulting flutter margin would not account for the true level of modeling errors. Stability measured with respect to globally derived uncertainty may be more conservative but this introduces a corresponding higher margin of safety.

Hybrid approaches are also formulated that mix the local and global approaches. One straightforward hybrid approach would be to generate an uncertainty description using all data from a small range of flight conditions. This approach may be useful for separately considering sets of plant models that are generated using different techniques. For example, the model-generating package used for this paper computes all subsonic plant models with a doublet-lattice algorithm, whereas the supersonic models are generating with constant pressure algorithms. A hybrid approach could be used to reflect this knowledge and consider groups of subsonic, supersonic, and transonic plants independently.

The approaches outlined here are certainly not exhaustive. A weighted norm approach can be formulated that uses flight data from the entire flight envelope, but depends heavily on a particular subset of that data. Other approaches could concentrate on particular dynamics through modal-filtering techniques to generate separate uncertainty descriptions for individual modes.[10]

Application: Robust Flutter Margins

Analytical Model

Robust flutter margins are computed for the F/A-18 Systems Research Aircraft (SRA), being flown at NASA Dryden Flight Research Center. The SRA is a two-seat F/A-18 fighter with production engines, but with a modified left wing involving aileron hinges and actuators larger than the standard equipment. A flight envelope had to be cleared for the F/A-18 SRA with this modification to ensure no aeroelastic instabilities would be encountered in flight.

A finite element model is coupled with an algorithm for computing the unsteady aerodynamic forces to compute a state-space representation of the aircraft dynamics. This model has 14 symmetric and 14 antisymmetric structural modes along with six rigid body modes. Stationary control surfaces are modeled in rig mode with static stiffness and damping associated with the actuator and hinge.

The model has an excitation force input that models the effects of a wingtip excitation system.[11] This force is assumed to excite only the symmetric modes or the antisymmetric modes separately. There are eight sensor measurements generated by accelerometers at the wingtip fore and aft, aileron, and stabilizer on each side.

Flight Data

Extensive flight data from the F/A-18 SRA is used to generate uncertainty descriptions for an analytical aircraft model. Over 30 flights were conducted in two sessions between September 1994 and February 1995 and between June 1995 and July 1995 at NASA Dryden Flight Research Center. Each flight performed maneuvers for different conditions throughout the flight envelope. A total of 260 different data sets are generated from conditions throughout the flight envelope ranging from altitudes up to 40,000 ft and Mach number up to 1.6.[12]

This flight data measures responses to a wingtip excitation system developed by Dynamic Engineering Incorporated (DEI) consisting of a wingtip exciter, an avionics box mounted in the instrumentation bay, and a cockpit controller.[13] The exciter generates forces rotating a slotted hollow cylinder around a small fixed aerodynamic vane. Rotating the cylinder varies the pressure distribution on the vane and results in a wingtip force changing at twice the cylinder rotation frequency. The magnitude of the resulting force is determined by the amount of opening in the slot.

The cockpit controller commands the frequency and magnitude of the wingtip forces. Frequency-varying excitation is generated by changing the cylinder rotation frequency with sine sweeps. The wingtip exciters are programmed to act in-phase (0 deg) or out-of-phase (90 deg) with each other. The in-phase sweeps are expected to excite the symmetric modes of the aircraft, whereas the out-of-phase sweeps should excite the antisymmetric modes.

Flight data sets are recorded by activating the exciter system at a given flight condition. The aircraft attempts to remain at the flight condition throughout the series of sine sweeps desired by the controller. The sine sweeps were restricted to within 3 and 35 Hz. Multiple sets of either linear or logarithmic sweeps were used with the sweep frequency increasing or decreasing.

Aeroelastic flight data generated with the DEI exciter system are analyzed by generating transfer functions from the excitation force to the sensor measurements using Fourier transform algorithms. The transient nature of this data violates several assumptions associated with Fourier analysis requiring stationary data composed of sums of infinite sinusoids. The analysis presented in this paper is based on Fourier analysis, although current research investigates wavelet techniques to analyze the flight data.[12]

Figure 3 presents an example of dynamical variations that are observed during flight testing. Two transfer functions generated from different data sets clearly show some variation in natural frequency even though each test point utilized the same sweep procedure at identical flight conditions of Mach 0.8 and 30,000 ft. One possibility to account for such variations is the change in mass, up to 10%, between the heavyweight and lightweight conditions as a result of fuel consumption. Another possibility is the nonideal phasing between the exciters causing excitation that is not purely symmetric.

The deviations between the modal response in Fig. 3 are used to generate uncertainty for the symmetric Wing 1st Bend-

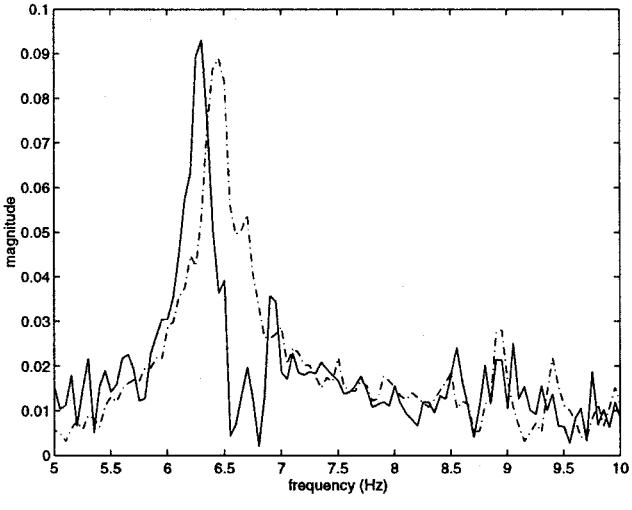

Fig. 3 Flight data transfer functions from symmetric excitation to left wing forward accelerometer for Mach = 0.8 and 30,000 ft demonstrating variation in modal frequency and damping.

ing mode. Similar deviations observed in modal responses are used to generate uncertainty for each mode. Uncertainty levels in modes that are not observed are assumed to be similar to those of the observed modes.

Additional uncertainty is required to account for behaviors resulting from improper exciter operation. The most noticeable of these improper behaviors occurred as a function of dynamic pressure. The motors and rotating cylinder assemblies would bind at high dynamic pressures causing erratic phase relationships between the individual exciters on opposite wingtips. Figure 4 shows a representative plot of the phase difference in degrees between the left and right exciters operating in symmetric mode for a sweep taken at a test point with $\bar{q}$ = 356 lb/ft^2. This phase plot, which does not maintain the desired 0-deg phase difference but is relatively constant and well behaved, is in direct contrast to the phase difference at a test point of $\bar{q}$ = 825 lb/ft^2 shown in Fig. 5.

Another improper behavior is the nonrepeatability observed with the data resulting from variations in transfer functions using different data sets recorded at identical flight conditions. An example of such a variation observed for frequency increasing and decreasing sweeps is shown in Figs. 6 and 7. The μ method is able to utilize the data despite these nonrepeatabilities that would adversely affect traditional system identification approaches.

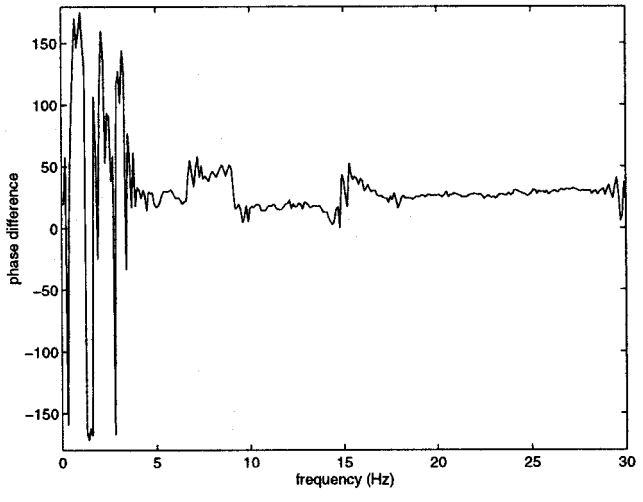

Fig. 4 Phase difference in degrees between left and right exciters for sweep range 3–30 Hz at Mach = 0.90 and 30,000 ft at $\bar{q}$ = 356 lb/ft^2.

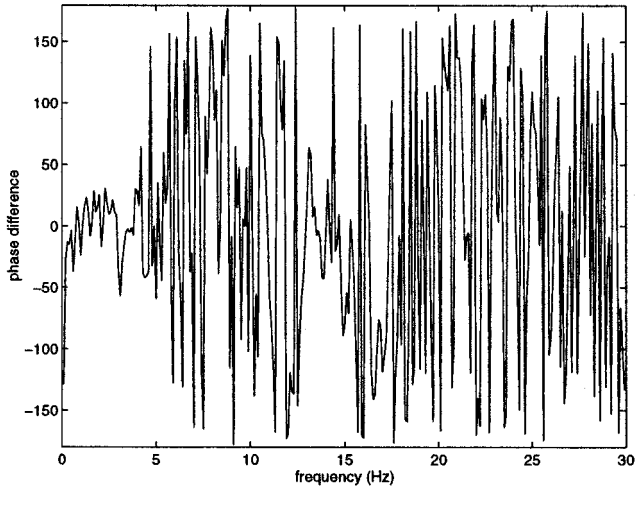

Fig. 5 Phase difference in degrees between left and right exciters for sweep range 3–30 Hz at Mach = 0.90 and 10,000 ft at $\bar{q}$ = 825 lb/ft^2.

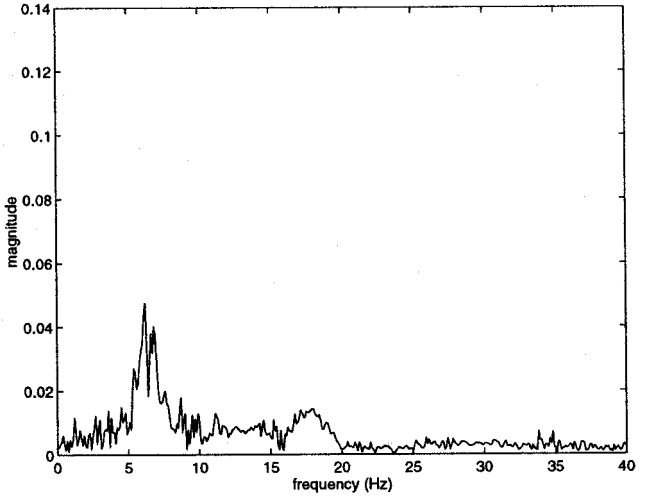

Fig. 6 Flight data transfer function from symmetric excitation to left wing forward accelerometer for Mach = 0.8 and 30,000 ft with frequency increasing sweep from 3–35 Hz.

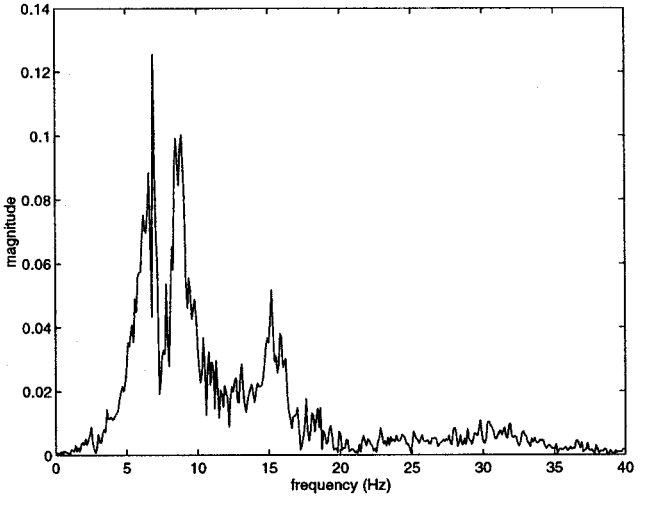

Fig. 7 Flight data transfer function from symmetric excitation to left wing forward accelerometer for Mach = 0.8 and 30,000 ft with frequency decreasing sweep from 3–35 Hz.

The data analysis process is further degraded by a poor measurement of the excitation force used to generate the modal responses. The excitation force is not directly measured, but rather a strain gauge measurement is used to approximate this force. The strain gauge records lateral shear strain at the exciter vane root that is assumed to be representative of the vertical shear and spanwise moment load at the wingtip rib.

The effect of the poor approximation to input force and the erratic behavior of the exciters is to reduce the quality of the flight data. Methods relying on system identification fail to accurately utilize the data to predict a flutter boundary, whereas the μ method is able to account for the data anomalies by including greater levels of uncertainty.

Uncertainty Description

An uncertainty description is associated with the theoretical model to account for errors and inaccuracies along with variations between the measured flight data transfer functions and predicted transfer functions. This description includes an operator describing parametric uncertainty in the modal parameters of the state matrix and another operator representing multiplicative uncertainty on the force input. A noise signal is included to affect the sensor measurements with a level of 10%.

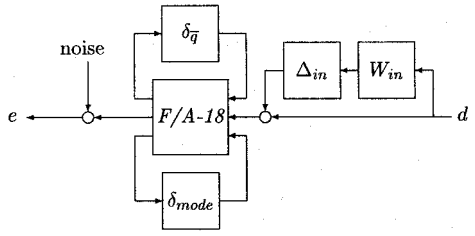

Fig. 8 F/A-18 SRA model with uncertainty.

A global approach is used to incorporate the flight data into this model by determining a single uncertainty description that is not invalidated by any of the multiple flight data sets. The operator magnitudes are the same for the model at different Mach numbers because the global approach formulates an uncertainty description that does not vary with flight condition. This description considers data from test points throughout the flight envelope, and so it is worst-case with respect to all of the measured data.

The parametric modal uncertainty Δ_A directly affects elements of the state matrix that is in a block diagonal form with natural frequency and damping values for each mode in distinct blocks. This uncertainty reflects errors in the static model and unmodeled time-varying modal changes caused by fuel consumption during flight. This uncertainty accounts for variations similar to those demonstrated in Fig. 3.

Separate operators are associated with each mode to distinguish between errors in natural frequency and damping. The same weightings are applied to all of the modes to assume each natural frequency can have the same level of error and each damping can have the same level of error. The model validation algorithms determine that no flight data invalidates the model if 5% uncertainty is associated with each natural frequency and 15% uncertainty is associated with each damping.

The low-frequency magnitude of the input multiplicative uncertainty Δ_{in} is chosen to ensure the model with the given amount of noise and parametric modal uncertainty is not invalidated. The high-frequency component reflects unmodeled dynamics in the linear model. W_{in} is the frequency-varying weighting for Δ_{in}:

$$W_{\text{in}} = 5\,\frac{s + 100}{s + 5000} \tag{22}$$

An additional parametric uncertainty δ_q is introduced to account for changes in flight condition and allow the model to describe the dynamics at a given Mach number for any value of dynamic pressure. Considering a perturbation to $\bar{q}$ in the equation of motion directly leads to formulation of the parametric uncertainty for computation of flutter margins.[9]

The block diagram for the aeroelastic model with the uncertainty operators is given in Fig. 8.

Robust Flutter Margins

Robust flutter margins are computed by analyzing the stability of the model with respect to the uncertainty description and the changes in flight conditions.[9] The smallest perturbation to dynamic pressure for which the model is not robustly stable to the entire set of uncertainty operators is the worst-case flutter margin. Symmetric and antisymmetric structural modes are considered separately for ease of presentation, but may be combined and analyzed as a single system.

Nominal flutter margins are initially computed by ignoring the modal and input uncertainties to determine the smallest destabilizing perturbation to dynamic pressure for the theoretical model. Robust flutter boundaries are computed with respect to the structured uncertainty set described in Fig. 8. The dynamic pressure associated with the flutter margins are converted into altitudes using standard atmospheric equations. These altitudes are plotted for the symmetric modes in Fig. 9 and for the antisymmetric modes in Fig. 10. A research flight envelope of the F/A-18 SRA is shown on these plots along with the required 15% flutter boundary for military aircraft.

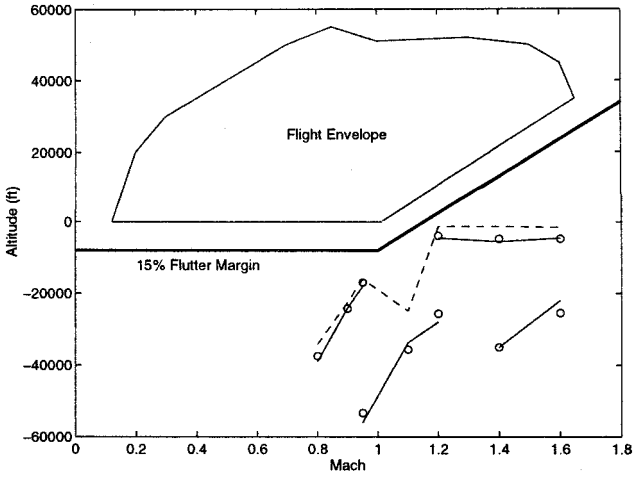

Fig. 9 Nominal and robust flutter points for symmetric modes: nominal *p-k* margin (——), nominal μ margin (○), robust μ margin (– – –).

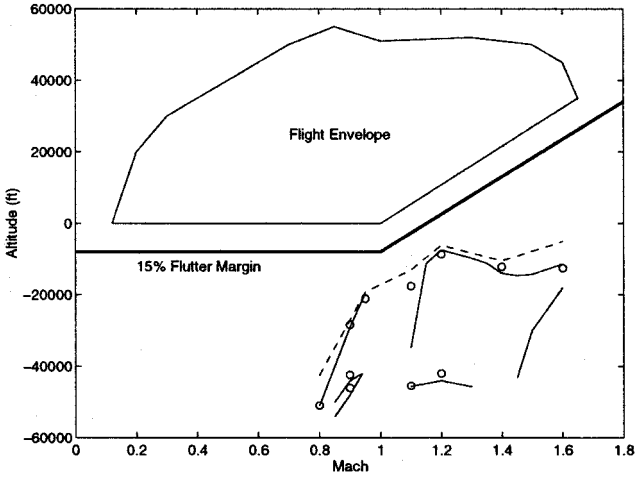

Fig. 10 Nominal and robust flutter points for antisymmetric modes: nominal *p-k* margin (——), nominal μ margin (○), robust μ margin (– – –).

Figures 9 and 10 use several short solid lines to indicate the *p-k* flutter solutions throughout the flight regime. Each of these short solid lines represents the flutter points caused by a specific mode. Circles represent the nominal flutter solutions computed using μ. A single dashed line represents the worst-case flutter margin at each flight condition computed from the robust model.

The robust flutter boundaries computed using μ have lower dynamic pressures than the nominal boundaries, which indicates the expected conservative nature of the robust computation. These new flutter points are worst-case values for the entire range of allowed uncertainty.

The flutter boundary at the transonic case, $M = 1.1$, demonstrates significant sensitivity to the modeling uncertainty. The dynamic pressures at flutter are approximately 70% for the robust flutter computation as compared to the nominal flutter boundary. The high sensitivity indicates that the analytical model must be extremely accurate at transonic for the predicted flutter margins to match the true margins; whereas the nominal *p-k* flutter margins do not indicate that extra caution must be taken at transonic flight.

The dark solid line on Figs. 9 and 10 represents the required boundary for flutter points. All nominal and robust flutter points lie outside this region, indicating the flight envelope should be safe from aeroelastic flutter instabilities. The robust flutter boundaries computed with μ indicate there is more danger of encountering flutter than was previously estimated with the *p-k* method. In particular, the robust flutter margin for symmetric excitation at $M = 1.2$ lies considerably closer to the boundary than the *p-k* method indicates.

Conclusions

This paper introduces a method of incorporating flight data into the development of an aeroelastic model. A robust stability framework is used that represents errors in the model by a set of norm-bounded operators. The flight data can be used to generate these operators and ensure that the model can account for the dynamics observed with multiple flight data sets. This method is advantageous as compared to system identification and parameter estimation methods for several reasons. Firstly, poor-quality data with low SNR can still be incorporated. Also, different levels of modeling errors estimated from different flights can be contained within the set of operators. Flight data from an F/A-18 is incorporated into a model using this method to generate robust flutter margins.

Acknowledgments

The authors acknowledge the financial support of the Structures Branch of NASA at Dryden Flight Research Center. Particular appreciation is extended to Larry Freudinger, Dave Voracek, Mike Kehoe, and Leonard Voelker. Rick Lind is supported through the Postdoctoral Fellowship program of the National Research Council.

References

[1]Ljung, L., *System Identification: Theory for the User*, Prentice–Hall, Englewood Cliffs, NJ, 1987.

[2]Kehoe, M., "A Historical Overview of Flight Flutter Testing," *Proceedings of the 80th AGARD Structures and Materials Panel*, CP-566, AGARD, 1995, pp. 1–15.

[3]Nissim, E., and Gilyard, G., "Method of Experimental Determination of Flutter Speed by Parameter Identification," NASA TP-2923, June 1989.

[4]Balas, G., Doyle, J., Glover, K., Packard, A., and Smith, R., *μ-Analysis and Synthesis Toolbox—Users Guide*, The MathWorks, Natick, MA, 1991.

[5]Packard, A., and Doyle, J., "The Complex Structured Singular Value," *Automatica*, Vol. 29, No. 1, 1993, pp. 71–109.

[6]Maciejowski, J., *Multivariable Feedback Design*, Addison–Wesley, Reading, MA, 1989.

[7]Kumar, A., and Balas, G., "An Approach to Model Validation in the μ Framework," *American Control Conference* (Baltimore, MD), Inst. of Electrical and Electronics Engineers, New York, 1994, pp. 3021–3026.

[8]Gupta, K., Brenner, M., and Voelker, L., "Development of an Integrated Aeroservoelastic Analysis Program and Correlation with Test Data," NASA TP-3120, May 1991.

[9]Lind, R., and Brenner, M., "Robust Flutter Margins of an F/A-18 Aircraft from Aeroelastic Flight Data," *Journal of Guidance, Control, and Dynamics*, Vol. 20, No. 3, 1997, pp. 597–604.

[10]Zhang, Q., Allemang, R., and Brown, D., "Modal Filter: Concept and Applications," *International Modal Analysis Conference* (Orlando, FL), Society for Experimental Mechanics, Bethel, CT, 1990, pp. 487–496.

[11]Vernon, L., "In-Flight Investigation of a Rotating Cylinder-Based Structural Excitation System for Flutter Testing," NASA TM-4512, June 1993.

[12]Brenner, M., Lind, R., and Voracek, D., "Overview of Recent Flight Flutter Testing Research at NASA Dryden," AIAA Paper 97-1023, April 1997.

[13]Reed, W., III, "A New Flight Flutter Excitation System," *Proceedings of the Society of Flight Test Engineers, 19th Annual Symposium* (Arlington TX), 1988.